Effect of variation of internal diameter along the length of a rotary kiln on material movement

E. R. Fedorova, *Candidate of Engineering Sciences, Department of Automation of Technological Processes and Productions*[1], *e-mail: apm_07_2@mail.ru*
V. V. Morgunov, *Post-Graduate Student, Department of Automation of Technological Processes and Productions*[1], *e-mail: vova.morgunov2011@yandex.ru*
E. A. Pupysheva, *Post-Graduate Student, Department of automation of Technological Processes and Productions*[1], *e-mail: elena.pupysheva1@gmail.com*

[1]*Empress Catherine II Saint Petersburg Mining University, Saint-Petersburg, Russia.*

Tubular rotary kilns are actively used in non-ferrous metallurgy, for example for sintering nepheline with limestone in alumina production. For the most effective heat exchange due to good mixing of the material in rotary kilns, a rolling regime characterized by the presence of an active layer and a stagnant area is maintained. Also the problem of formation of coating layers inside the kiln, which leads to a narrowing of the inner diameter of the aggregate, is known. In this paper, using the DEM-modeling method the influence of limes on the active layer parameters: the average speed of particles in the active layer and the share of the active layer in the aggregate at different rotational speeds and the degree of filling of the drum. With the increase of the coating layers thickness the average speed of particles in the active layer and the proportion of particles in the active layer in the entire profile of the kiln increases, changes in the shape of the profile of the speed of particles in the active layer and the proportion of particles in the active layer, depending on the thickness of coating layers are observed. The obtained conclusions are of qualitative nature and indicate a significant influence of the coating layers thickness on the active layer parameters and the need for further study of this process on the physical model with the real charge material.

Key words: alumina, nepheline, tube kilns, material motion, rotating cylinder, active layer, particle motion, coating layers, DEM, numerical simulation.

DOI: 10.17580/nfm.2024.01.05

Introduction

Tube Rotary Kilns (TRK) are used extensively in metallurgy and other industries [1].

The furnace is a solid steel rotating cylinder inclined at a slight angle to the horizon. The upper part is continuously fed with material, which due to the inclination and rotation moves to the lower part of the kiln, where a burner is located, the hot gas from which moves countercurrently to the material.

Despite the differences in the processes occurring in the TRK, there are a number of features of the unit, which significantly complicate the control of this object: multi-connectedness of input and output parameters of the object; high correlation of input parameters among themselves; high temperatures required for the process; a large number of perturbing influences [2–4]; high inertia and lag in most control channels. At present used automation systems are characterised by separate loops of input parameters stabilisation, the purpose of the whole system is to stabilise the temperature profile in the range specified by the regulations, in idealised conditions of process control – to maintain a narrow temperature range in the sintering zone.

A promising direction of development of process automation is advanced control or APC-technology [5–7]. This type of control assumes the presence of an adequate robust model of the control object implemented as an add-on under the SCADA-system. Control by the model can be carried out in the "advisor" mode or in the online control mode [8, 9]. However, at the moment in the world scientific literature there are no models that would allow to get such a high-precision representation of the processes in the given aggregate.

Speaking about material motion in the TRK, it is necessary to refer to the topic of bulk material motion in tubular rotating cylinders. Rotating cylinders include not only TRKs but also other industrial units: ball mills, refrigerators, dryers, mixers, etc. According to the literature, the motion in a rotating cylinder (including TRKs) can be roughly divided into two components: axial motion and transverse motion.

Axial motion is the movement of material along the axis of the kiln, i.e. from the loading point to the discharge point. This component usually takes into account parameters such as the residence time of the material in the furnace, the mass flow rate of the material in the axial direction, the profile of the height of the material layer, and the profile of the degree of filling.

Transverse motion is the description of the material motion in the transverse plane of the kiln. The most

fundamental works on this subject are the work of Henein [10] and the continuing work of Mellman [11], which describe 7 basic modes of material motion formed as a function of Froude number, filling factor and friction coefficient. The rolling mode is the most characteristic mode of motion for the TRK. The material motion in this mode is characterised by the following properties: the material is divided into two regions: a passive region and an active layer, with intensive mixing in the active layer and a relatively flat material surface.

This work aims to investigate the effect of varying the internal diameter of a rotating cylinder simulating the formation of coating layers on the parameters of the transverse motion of bulk material. The aim of this work is to analyse the effect of the coating layers on the average transverse velocity of particles in the active layer and the proportion of material in the active layer at different rotational speeds and the degree of loading of the drum in the rolling mode. The stated problem was labelled as essential in the works of many authors [12–14], but was not supported by experiments and calculations in software products. This study is qualitative in nature.

Methods

The DEM numerical modelling method based on the commercial software Rocky DEM was used to simulate the movement of bulk materials.

More details on this modelling method can be found in [15, 16], as well as examples of the use of numerical modelling methods in metallurgy, electrolysis processes [17, 18], energy [19, 20] and oil industry [21].

The most important role in the process of numerical DEM modelling is the calibration of material properties [22, 23]. For the topic of this study, the most significant parameter is the dynamic slope angle of the material, and the particles were calibrated according to it. Glass spheres were chosen as the material due to the availability of a large amount of experimental data in the literature, as well as the relatively small time required for modelling due to the sphericity of the particles. The calibration parameters were adopted according to the publication [24], where the authors presented a table of real experiments, the results of the DEM modelling process, as well as graphical material on the results of experiments and DEM modelling. The material calibration in [24] was carried out in a drum with the parameters: drum diameter 100 mm, drum length 100 mm, filling degree 20%, rotation speed 14.32 rpm, particle diameter 3.68 mm.

Based on the results presented in [24], DEM modelling with similar parameters was carried out. The dynamic slope angle of the material was 31.2 degrees, which is in agreement with the experimental and modelled values in [24] and [25].

The values of drum rotation speed and filling degree were chosen as basic values, and they were varied in the ranges investigated in [24].

Table 1 presents the parameters at which the subsequent modelling was carried out.

Based on the work of [26], four types of geometry simulating a coating layers were prepared by analogy. The geometry was constructed according to the following principle: a truncated cone with a length of 660 mm was inserted into a cylinder with a diameter of 200 mm and a length of 1000 mm; the diameter of the cone and, accordingly, the angle of inclination of its walls were varied. This design allows us to show the non-uniformity of the formation of coating layers in the kiln. For example, in the last cooling zone at a given furnace operation mode, the coating layer is not formed, while the most probable place of its appearance is the sintering zone. The geometry was constructed in Ansys SpaceClaim software. **Table 2** shows the characteristics of all geometry types and **Fig. 1** shows the geometry itself.

In order to analyze the particle motion inside the kiln, taking into account the geometry of the kiln, it was divided into sections **(Fig. 2)**. The division was made according to the following principle: at the beginning and the end of the kiln, two small zones of 100 mm each

Table 1
Modeling parameter

Parameters	Values	Measurement units
Particle density	2460	kg/m^3
Static particle-particle friction	0.1	–
Dynamic particle-particle friction	0.1	–
Particle-particle recovery coefficient	0.81	–
Static friction particle-drum	0.23	–
Dynamic particle-drum friction	0.23	–
Particle-drum recovery coefficient	0.3	–
Particle diameter	3.68	mm
Drum diameter	200	mm
Drum length	1000	mm
Calculation algorithms		
Normal force	Hysteretic Linear Spring	
Tangential force	Linear Spring Coulomb Limit	
Adhesion strength	Absent	
Gravity	9.81 m/s^2	
Impact energy	By default	
Rolling resistance model	Absent	

Table 2
Geometry parameters

Type	Wall accretion thickness (mm)	Effective diameter at 66% of length (%)	Closed diameter by 66% of length (%)	Cone wall angle (0)
0	0	100	0	0
1	5	90	10	0.43
2	15	70	30	1.30
3	25	50	50	2.17

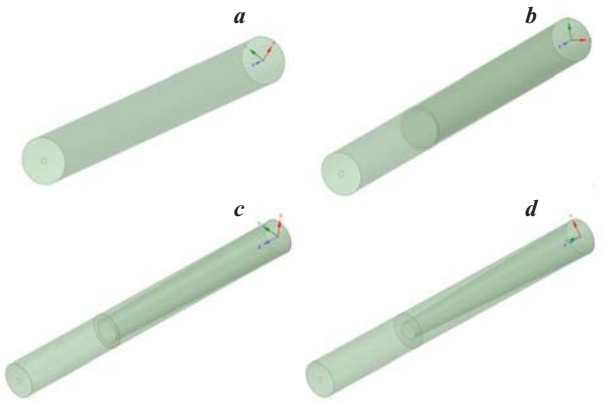

Fig. 1. Types of geometry (*a* – Type 0, *b* – Type 1, *c* – Type 2, *d* – Type 3)

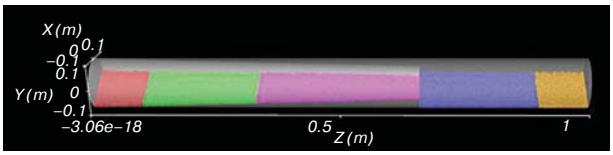

Fig. 2. Division of the drum into regions for the analysis of geometry features: Zone 1 – red; Zone 2 – green; Zone 3 – purple; Zone 4 – blue; Zone 5 – orange

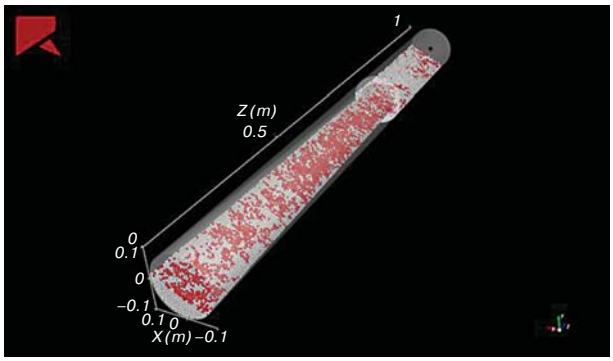

Fig. 3. Defining the boundary velocity

(Zones 1, 5), where the particle motion will be most significantly affected by the wall effect, were selected. Two zones (Zones 2, 3) were also identified where coating layers were present. It is assumed that in Zone 2 the influence of coating layer will be much lower than in zone No. 3 due to the difference in effective diameter in these zones. The length of Zone 2 is 230 mm and Zone 3 is 330 mm. The last section is Zone 4 with a length of 240 mm — a section free of coating layer.

Thus, for each of the four types of geometry (**Table 2**), modelling was carried out by varying two different parameters: drum speed and filling degree. When the drum speed was varied (14.32; 16.32; 18.32 (rpm)), the drum fill degree was kept constant for all iterations (20.01%). When the drum filling degree was varied (20.01%, 17.98%, 16.08%), the drum rotation speed was kept constant for all iterations (14.32 rpm). The selected values of rotation speed and degree of drum filling are not equal to the values of real TRK, but the main task in selecting the ranges of these parameters is to obtain the mode of movement of bulk material characteristic of TRK — rolling mode.

Two parameters were determined: the average transverse velocity of particles in the active layer and the proportion of material in the active layer. To distinguish between two areas (passive region and active layer) it was decided to introduce some boundary velocity, selected separately for each set of values of input parameters, when reaching which it is considered that the particle is in the region of the active layer.

The boundary velocity was determined using the Rocky DEM visualisation tools. The boundaries of the color scale representing the particle velocity were empirically selected to allow binarisation of particles inside the drum, the boundary of binarisation being the desired boundary velocity **(Fig. 3)**.

Results

In this paper, the effect of drum geometry features on the average transverse velocity of particles in the active layer and the fraction of material in the active layer at different drum speeds and degrees of drum filling was investigated.

Further, all graphs **(Fig. 4)** use the same lines to indicate certain types of geometry.

The analysis of the graphs (**Fig. 4**) is presented in the form of a table. The table is divided into 4 parts, in each of which one specific graph is analyzed. The rows of the table show the types of geometry corresponding to **Table 2**. The columns of the table show the variation of the operating parameter (rotational speed or filling degree, according to the research methodology). The cells of the table show 3 types of information. Under numeral one is given a qualitative description of the postonal comparison of the value of the investigated parameter in the geometry with constriction and given operating parameters with the value of the investigated parameter in the absence of constriction in the geometry, but with similar operating conditions. Under numerical two, a qualitative description of the effect of the geometry is given in comparison to iterations with other operating parameters. At the end of each cell, the change of the investigated parameter with respect to the values inherent to the zero type of geometry with the same operating parameters is presented by zone.

Discussion

DEM modelling has produced qualitative results representing the distribution profile of the number of particles in the active layer and the average velocity in the active layer along the length of a rotating cylinder with local variation of the inner diameter, simulating coating layer formation. The data obtained provide an initial insight into the nature of material movement in the presence of coating layers.

Glass spheres with a diameter of 3.68 mm were chosen as this material was used not only in [24], which was used for calibration in this study, but also appeared in at

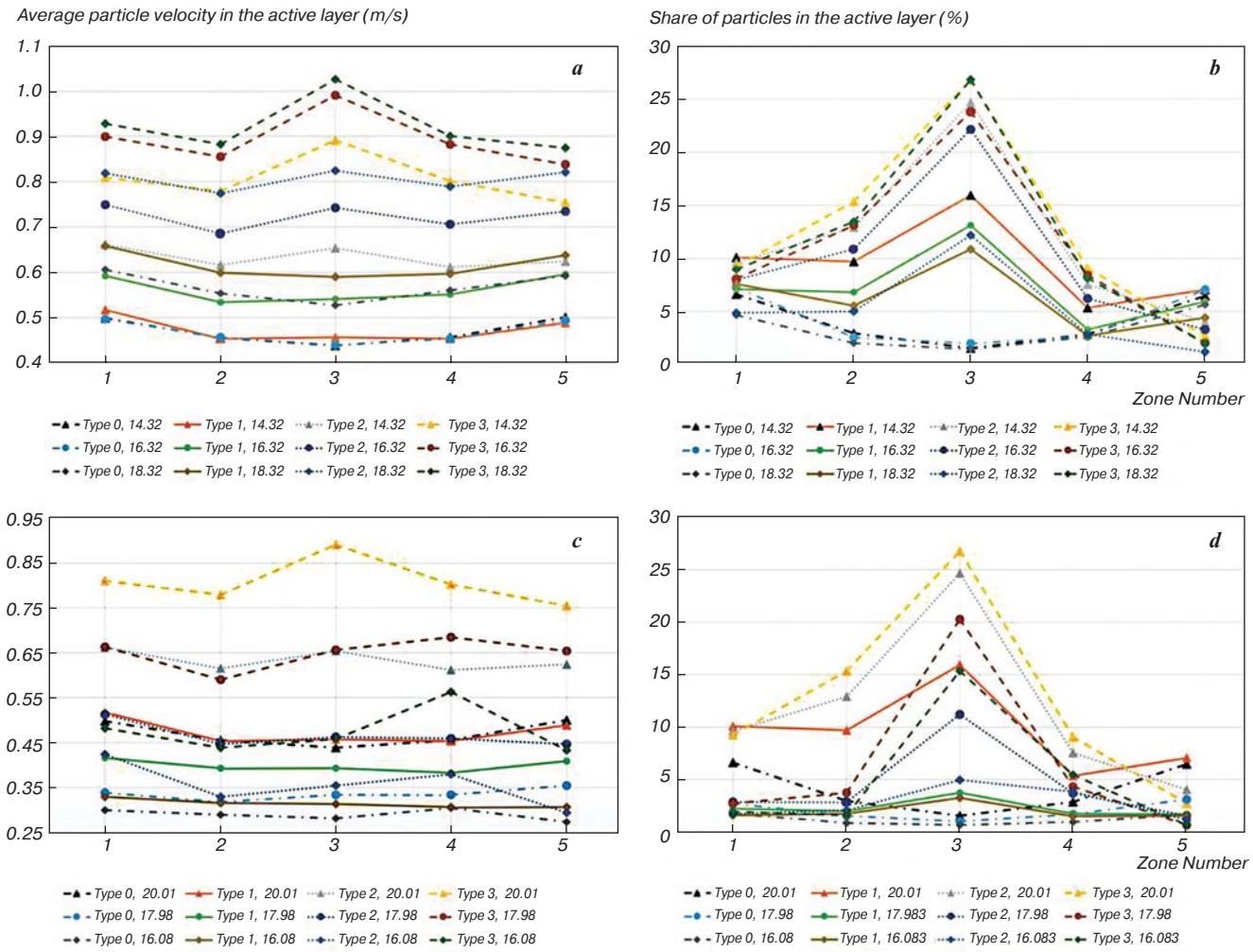

Fig. 4. Profile of average transverse velocity of particles in the active layer (*a*, *b*) and number of particles in the active layer (*c*, *d*) under conditions of different types of geometry when changing the drum rotation speed (*a*, *c*) and the degree of drum filling (*b*, *d*)

Table 3
Description of results

Influence of coating layer thickness on the average transverse velocity of particles in the active layer at different drum rotation speeds (Fig. 4, *a*.).			
GT/PV*	14.32 rpm	16.32 rpm	18.32 rpm
0	Zones 1 and 5 — elevation due to wall effect, straight profile; lack of coating layers		
1	1. Minor changes compared to geometry type 0	1. Equal increase in all zones. 19.2%, 17.1%, 22.9%, 21.3%, 20.3%	1. Equal increase in all zones. 2. Effect of geometry below the 16.32 rpm variant. 10.6%, 10.0%, 14.5%, 7.9%, 9.1%
2	1. Increase in all zones. Peak in zone 3. 32.8%, 35.2%, 49.2%, 34.1%, 24.6%	1. Increase in all zones. Peak in zone 3. 2. Influence of geometry above the variant with 14.32 rpm. 50.7%, 50.4%, 69.1%, 55.4%, 47.9%	1. Increase in all zones. Peak in zone 3. 2. The effect of geometry is similar to the 16.32 rpm variant. 42.8%, 48.6%, 68.0%, 50.1%, 45.7%
3	1. Increase in all zones. Peak in zone 3. 2. Effect of constriction higher than in Type 2 geometry. 62.6%, 71.2%, 103.3%, 75.8%, 50.7%	1. Increase in all zones. Peak in zone 3. 2. Influence of geometry above the variant with 14.32 rpm. 80.8%, 87.7%, 125.7%, 94.1%, 68.8%	1. Increase in all zones. Peak in zone 3. 2. Effect of geometry below the 16.32 rpm variant. 64.9%, 72.4%, 114.1%, 74.6%, 56.5%

Table 3 continued

Influence of coating layer thickness on the fraction of particles in the active layer at different drum rotation speeds (Fig. 4, *b*).			
GT/PV	14.32 rpm	16.32 rpm	18.32 rpm
0	Zones 1 and 5 — elevation due to wall effect, straight profile; lack of coating layers		
1	1. Increase in all zones. Peak in zone 3. 51.9%, 229.8%, 925.3%, 86.5%, 9.3%	1. Increase in zones 2–4. Decrease in zones 1 and 5. Peak in zone 3. 2. Effect of geometry below the 14.32 rpm variant. –1.6%, 164.1%, 559.6%, 22.9%, –16.1%	1. Increase in zones 1–4. Decrease in zone 5. Peak in zone 3. 2. Effect of geometry above the 16.32 rpm variant. 62.3%, 171.4%, 663.8%, 4.8%, –21.8%
2	1. Increase in zones 1–4. Decrease in zone 5. Peak in zone 3. 2. Effect of narrowing higher than in Type 1 geometry. 44.4%, 339.7%, 1485.9%, 161.2%, –37.4%	1. Increase in zones 1–4. Decrease in zone 5. Peak in zone 3. 2. Effect of geometry below the 14.32 rpm variant. 10.4%, 319.6%, 1015.3%, 133.3%, –53.3%	1. Increase in zones 1–4. Decrease in zone 5. Peak in zone 3. 2. Effect of geometry below the 16.32 rpm variant. 3.5%, 145.7%, 756.4%, 10.7%, –78.7%
3	1. Increase in zones 1–4. Decrease in zone 5. Peak in zone 3. 2. Effect of narrowing higher than in Type 2 geometry 39.8%, 422.4%, 1620.4%, 214.8%, –57.9%	1. Increase in zones 1–4. Decrease in zone 5. Peak in zone 3. 2. Effect of geometry below the 14.32 rpm variant. 11.8%, 406%, 1098%, 216.8%, –71%	1. Increase in zones 1–4. Decrease in zone 5. Peak in zone 3. 2. Effect of geometry above the 16.32 rpm variant. 90.9%, 558.2%, 1787.3%, 211.6%, –65%.
Influence of coating layers thickness on the average transverse velocity of particles in the active layer at different degrees of drum filling (Fig. 4, *c*)			
GT/PV	20.01%	17.98%	16.08%
0	Zones 1 and 5 — elevation due to wall effect, straight profile; lack of coating layers		
1	1. Minor changes compared to type 0	1. Equal increase in all zones 22.8%, 23.5%, 17.6%, 14.9%, 15.2%	1. Equal increase in all zones. 2. Influence of geometry below the variant with 17.98% 9.7%, 9.24%, 11.2%, 0.5%, 12.5%
2	1. Equal increase in all zones. 32.9%, 35.2%, 49.2%, 34.1%, 24.6%	1. Increase in all zones. 2. The influence of geometry decreases in zone 3 and increases in the other zones compared to the variant 20.01%. 51.3%, 40.7%, 38.4%, 37.5%, 25.8%	1. Increase in all zones. 2. Impact of geometry below the variant with 17.98% 41.4%, 14%, 25.6%, 24.5%, 7.7%
3	1. Increase in all zones. Peak in zone 3. 2. Effect of constriction higher than in Type 2 geometry. 62.6%, 71.2%, 103.3%, 75.8%, 50.5%	1. Increase in all zones. 2. Influence of geometry above the variant with 20.01% 95.7%, 85.8%, 96.5%, 105.2%, 84.4%	1. Increase in all zones. Peak in zone 4. 2. Effect of geometry below the variant with 17.98% 60.8%, 51.8%, 62.4%, 84.8%, 58.5%
Influence of coating layers thickness on the fraction of particles in the active layer at different degrees of drum filling (Fig. 4, *d*)			
GT/PV	20.01%	17.98%	16.08%
0	Zones 1 and 5 — elevation due to wall effect, straight profile; lack of coating layers		
1	1. Increase in all zones. Peak in zone 3. 51.9%, 229.8%, 925.3%, 86.5%, 9.3%	1. Increase in zones 2–4. Decrease in zone 1.5. Peak in zone 3. 2. The influence of geometry is lower compared to the variant 20.01%. –18.9%, 29.4%, 262.3%, 1.9%, –44.9%	1. Increase in zones 2-4. Decrease in zone 1.5. Peak in zone 3. 2. Effect of geometry is higher in zones 2–4, lower in zones 1 and 5 compared to the variant 17.98%. –5.8%, 100%, 390.6%, 54.3%, –5.1%+
2	1. Increase in zones 1–4. Decrease in zone 5. Peak in zone 3. 2. Effect of narrowing higher than in Type 1 geometry. 44.4%, 339.7%, 1485.9%, 161.2%, –37.4%	1. Increase in zones 1–4. Decrease in zone 5. Peak in zone 3. 2. The influence of geometry is lower compared to the variant 20.01%. 4%, 83.1%, 989.7%, 199.2%, –50.4%	1. Increase in zones 1–4. Decrease in zone 5. Peak in zone 3. 2. The influence of geometry is lower compared to the variant 17.98%. 4%, 83.1%, 989.7%, 199.2%, –50.4%
3	1. Increase in zones 1–4. Decrease in zone 5. Peak in zone 3. 2. Effect of narrowing higher than in Type 2 geometry. 39.8%, 422.4%, 1620.4%, 214.8%, –57.9%	1. Increase in zones 2–4. Decrease in zone 5. No change in zone 1. Peak in zone 3. 2. Effect of geometry zones 1,2,4 lower compared to the variant 20.01%. –0.6%, 142.6%, 1872.5%, 156.1%, –79.1%	1. Increase in zones 1–4. Decrease in zone 5. Peak in zone 3. 2. Effect of geometry is higher in zones 1,3,4 compared to the variant 17.98%. 11.5%, 84.1%, 2228.5%, 462.3%, –58.2%

*GT – geometry type, PV – parameter value

least three other papers that performed its CFD modelling and PEPT experiments [27–29]. Also, [27] presented a methodology for verifying the CFD model results using experimental data from [29]. For this purpose, a transverse slice was used in which the transverse velocity along the height of the material layer was considered. Specifically for this comparison, a separate iteration of the simulation was performed at the parameters: cylinder speed 13.85 rpm and filling degree 18.81%. The results showed high convergence with the data in [27–29].

The differences between the values obtained from the modelling and the experimental data from are within the error range specified in [29]. Thus, it can be said that the DEM model was verified on the results of a real experiment presented in the scientific literature.

The presented study is part of a larger project to develop a predictive control system for TRK for sintering nepheline concentrate with limestone. This system is expected to result in an increase in alumina recovery from 88% to 91% by maintaining a more efficient sintering site temperature range of 1275–1300 °C. The methodology from [30] was used to calculate the economic efficiency of the project. The results obtained can be used at the Pikalevsky and Achinsk alumina refineries. Within the framework of the project the following economic indicators were calculated: NPV = 118 million rubles, PI = 1.2 rubles, and the discounted payback period was 2 years and 5 months. Based on the calculated indicators, investments in the proposed project can be considered economically feasible.

Conclusion

In this study, a geometry was constructed to simulate the formation of a coating layer inside a tubular kiln based on the methodology presented in [26]. This geometry was used for numerical DEM modelling of the motion of glass spheres in a rotating drum. As a result, profiles along the length of the drum of the average transverse velocity of particles in the active layer and the fraction of particles in the active layer at different values of the drum rotation speed and the degree of filling of the drum were obtained. It was possible to verify the modelling results by comparing the transverse profile of the particle velocity with the real experiment data presented in [25]. On the basis of the obtained data it was possible to draw the following qualitative conclusions:

1. The influence of the drum geometry on the transverse velocity of particles in the active layer at different cylinder rotation speed. As the rotational speed increases, an increase in the relative velocity is first observed, followed by a decrease at a value of 18.32 rpm, which is true for all types of geometry investigated.

2. Effect of drum geometry on the transverse velocity of particles in the active layer at different filling degree of the cylinder. As the filling degree decreases, firstly an increase in the relative velocity is observed and then a decrease occurs at a value of 16.08 %, which is true for all types of geometry investigated.

3. The influence of geometry has a non-linear character on the number of particles in the active layer at different values of rotational speed and cylinder filling degree. In some zones there is a decrease in the fraction of particles relative to zero geometry.

4. With the appearance of coating layers and increase in their thickness, the character of the profile of the mean transverse velocity profile of particles in the active layer changes. In particular, in the sections of the drum profile where coating layers are present, the increase in the average transverse velocity of particles in the active layer is much more pronounced as the thickness of the coating layer increases. However, when the drum filling degree decreases, a change in the profile with an increase in the average transverse velocity of particles in the active layer was observed in the section free of coating layer, but adjacent to it. It is assumed that at decreasing the degree of drum filling the most significant contribution to the velocity distribution was made by the wall effect in this section.

5. With the appearance of coating layer and increase of its thickness, the character of the profile of the particle fraction in the active layer changes. In particular, in the sections of the drum profile where coating layers are present, the increase in the fraction of particles in the active layer with increasing thickness of the coating layer is much more pronounced.

6. The presence of walls at the inlet and outlet of the drum has the most active effect on the average transverse velocity of particles in the active bed and the fraction of particles in the active bed in the immediate vicinity of them.

The qualitative conclusions presented in the paper show that the change in the internal diameter of a rotating cylinder can have a significant effect on the movement of bulk material, both in the zones of diameter contraction and along the entire length of the cylinder and requires further comprehensive study.

References

1. Anisonyan K. G., Kopyev D. Yu., Olyunina T. V., Sadykhov G. B. Influence of Na_2CO_3 and $CaCO_3$ Additions on the Aluminate Slag Formation During a Single-Stage Reducing Roasting of Red Mud. *Non-ferrous Metals*. 2019. No. 1. pp. 17–21.

2. Petrov P. A., Shestakov A. K., Nikolaev M. Yu. Use of Multifunctional Crust Breaker and Machine Vision System for Acquisition and Processing of Aluminium Reduction Cell Data. *Tsvetnye Metally*. 2023. No. 4. pp. 45–53.

3. Shestakov A. K., Petrov P. A., Nikolaev M. Y. Automatic System for Detecting Visible Emissions in a Potroom of Aluminum Plant Based on Technical Vision and a Neural Network. *Metallurgist*. 2023. Vol. 66, Iss. 9-10. pp. 1308–1319.

4. Bazhin V. Yu., Masko O. N., Martynov S. A. Automatic Burden Balance Monitoring and Control in the Production of Metallurgical Silicon. *Tsvetnye Metally*. 2023. No. 4. pp. 53–60.

5. Machalek D., Powell K. M. Model Predictive Control of a Rotary Kiln for Fast Electric Demand Response. *Minerals Engineering*. 2019. Vol. 144. 106021.

6. Zubov V. P., Yunpeng L. Slicing Mining of Thick Gently Dipping Coal in China: Problems and Improvement. *MIAB*. 2023. Iss. 7. pp. 37–51.

7. Bazhin V. Yu., Masko O. N., Nguyen Huy H. Increasing the Speed of Information Transfer and Operational Decision-Making in Metallurgical Industry Through an Industrial Bot. *Non-ferrous Metals*. 2023. No. 1. pp. 62–67.

8. Rozhkov V. V., Krutikov K. K., Fedulov A. S., Fedotov V. V. Simulation of Induction Motors with Energy Recuperation for Lifting Mechanisms of Non-Ferrous Metallurgy Enterprises. *Non-ferrous Metals*. 2021. No. 1. pp. 74–80.

9. Pancnehko S. V., Dli M. I., Bykov A. A. Simulation and Algorithmization of Analysis of Heat and Mass Transfer Processes in Chemical Electrothermy Units in Non-Ferrous Metallurgy. *Non-ferrous Metals*. 2022. No. 1. pp. 46–54.

10. Henein H., Brimacombe J. K., Watkinson A. P. Experimental Study of Transverse Bed Motion in Rotary Kilns. *Metallurgical Transactions B*. 1983. Vol. 14, Iss. 2. pp. 191–205.

11. Mellmann J. The Transverse Motion of Solids in Rotating Cylinders-Forms of Motion and Transition Behavior. *Powder Technology*. 2001. Vol.118, Iss. 3. pp. 251–270.

12. Pieper C., Wirtz S., Schaefer S., Scherer V. Numerical Investigation of the Impact of Coating Layers on RDF Combustion and Clinker Properties in Rotary Cement Kilns. *Fuel*. 2021. Vol. 283. 118951.

13. Khodorov E. I. Cement Industry Furnaces. 2nd ed., revised. Leningrad: Stroyizdat, 1968. 456 p.

14. Mujumdar K. S., Ranade V. V. CFD modeling of rotary cement kilns. *Asia-Pacific Journal of Chemical Engineering*. 2008. Vol. 3, Iss. 2. pp. 106–118.

15. Cundall P. A., Strack O. D. L. A Discrete Numerical Model for Granular Assemblies. *Géotechnique*. 1979. Vol. 29, Iss. 1. pp. 47–65.

16. Moncada M., Toledo P., Betancourt F., Rodríguez C. G. Torque Analysis of a Gyratory Crusher with the Discrete Element Method. *Minerals*. 2021. Vol. 11, Iss. 8. 878.

17. Ilyushin Y. V., Martirosyan A. V. The Development of the Soderberg Electrolyzer Electromagnetic Field's State Monitoring System. *Scientific Reports*. 2024. Vol. 14. 3501.

18. Kukharova T.V., Ilyushin Y. V., Asadulagi M. M. Investigation of the OA-300M Electrolysis Cell Temperature Field of Metallurgical Production. *Energies*. 2022. Vol. 15, Iss. 23. 9001.

19. Shklyarskiy Y. E., Skamyin A. N., Jiménez Carrizosa M. Energy Efficiency in the Mineral Resources and Raw Materials Complex. *Journal of Mining Institute*. 2023. Vol. 261. pp. 323–324.

20. *Skamyin A., Shklyarskiy Ya., Lobko K., Dobush V., Sutikno T., Jopri* M. H. Impedance Analysis of Squirrel-Cage Induction Motor at High Harmonics Condition. *Indonesian Journal of Electrical Engineering and Computer Science*. 2024. Vol. 33, Iss. 1. pp. 31–41.

21. Korobkov G. E., Yanchushka A. P., Zakiryanov M. V. Numerical Modeling of a Stress-Strain State of a Gas Pipeline with Cold Bending Offsets According to in-Line Inspection. *Journal of Mining Institute*. 2018. Vol. 234. pp. 643–646.

22. Sebastian Escotet-Espinoza M., Foster C. J., Ierapetritou M. Discrete Element Modeling (DEM) for Mixing of Cohesive Solids in Rotating Cylinders. *Powder Technology*. 2018. Vol. 335. pp. 124–136.

23. Hlosta J., Jezerská L., Rozbroj J., Žurovec D., Nečas J., Zegzulka J. DEM Investigation of the Influence of Particulate Properties and Operating Conditions on the Mixing Process in Rotary Drums: Part 2-Process Validation and Experimental Study. *Processes*. 2020. Vol. 8, Iss. 2. 184.

24. Santos D. A. Investigation of Particle Dynamics in a Rotary Drum by Means of Experiments and Numerical Simulations Using DEM. *Advanced Powder Technology*. 2016. Vol. 27, Iss. 2. pp. 692–703.

25. Xiao Y. L., Specht E., Mellmann J. Experimental Study of the Lower and Upper Angles of Repose of Granular Materials in Rotating Drums. *Powder Technology*. 2005. Vol. 154, Iss. 2-3. pp. 125–131.

26. Chatterjee A., Mukhopadhyay P. K. Flow of Materials in Rotary Kilns Used for Sponge Iron Manufacture: Part III. Effect of Ring Formation Within the Kiln. *Metallurgical Transactions B*. 1983. Vol. 14, Iss. 3. pp. 393–399.

27. Zheng X., Jin B., Zhang Y., Zhang Y., Zhou C. Numerical Simulation of Flow Characteristics in an Inclining Rotating Kiln with Continuous Feeding. *International Journal of Chemical Reactor Engineering*. 2019. Vol. 17, Iss. 10. 20180203.

28. Scatena R., Ferreira L. C., Santos D. A., Duarte C. R., Barrozo M. A. S. Tambor Rotatório Operando No Regime De Rolamento: Um Estudo Experimental E Numérico. *Anais Do XX Congresso Brasileiro de Engenharia Química*. 2015. pp. 6305–6312.

29. Santos D. A., Petri I. J., Duarte C. R., Barrozo M. A. S. Experimental and CFD Study of the Hydrodynamic Behavior in a Rotating Drum. *Powder Technology*. 2013. Vol. 250. pp. 52–62.

30. Alexandrov A. V., Nemchinova N. V. Calculation of the Expected Economic Efficiency of Aluminum Production by Increasing the Use of Alumina of Domestic Production. *Proceedings of Irkutsk State Technical University*. 2020. Vol. 24. pp. 408–420. NFM